

THE UNIVERSITY OF MICHIGAN
College of Engineering
Department of Mechanical Engineering
Cavitation and Multiphase Flow Laboratory

Report No. U-MICH 01357-17-T

PRELIMINARY COULTER-COUNTER MEASUREMENTS IN
HIGH SPEED CAVITATION TUNNEL

by

O. Ahmed
N. R. Bhatt
F. G. Hammitt

Financial Support Provided by:

National Science Foundation

Grant No. GK-1889

June 1970

ACKNOWLEDGEMENTS

The authors express their gratitude to Mr. E. E. Timm, a Doctoral candidate at the University of Michigan for the assistance he gave in building the pulse shaper used in this work.

LIST OF FIGURES

Figure		Page
1.	Schematic of Water Tunnel Test Facility	15
2.	Photograph of Water Tunnel Test Facility	16
3.	Venturi Test Section	17
4.	Schematic of Sampling Line	18
5.	Schematic of Pressure Chamber	19
6.	Photograph of Coulter Tube	20
7a.	Particle Passing Through the Orifice	21
7b.	Section of an Element of the Orifice with a Part of the Particle Passing Through It	21
8.	Block Diagram of the Electric Instruments Used in Test	22
9.	Photograph of Complete Set-Up	23
10.	Shape of the Pulse for the Pulse Shaper	24
11a.	Circuit Diagram of the Pulse Shaper	25
11b.	Continued	26
11c.	Continued	27
12.	The 128 Multichannel Analyzer	28
13.	The Form of the Output Spectrum of the Multichannel Analyzer	29
14.	The Input Pulses to the Pulse Shaper Together with its Output Pulses	30
15.	The Linearity Checking Results of the Pulse Shaper	31
16.	The Linearity Checking Results of the Multichannel Analyzer	31
17.	The Size Distribution of Ragweed Particles at Different Gain Settings	32
18a.	The Size Distribution of Latex Particles at Different Gain Settings	33
18b.	Continued	34
19.	Calibration Curve of the Set-Up for Size Measurements at Different Gain Settings	35

Figure	Page
20. Nuclei Size Distribution of the Tunnel Water at Different Times	36
21. The Entrained Gas Content as a Function of Time	37

I. INTRODUCTION

Bubble nucleation in a liquid, in either a cavitation or boiling situation depends primarily on the concentration and distribution of gas and vapor nuclei. Several techniques have been utilized in the past to attain data on the size and spatial distribution of these nuclei. For example their effects upon acoustic and light transmission have been investigated. These techniques provide information which is incomplete in various different ways, they are complex and they usually involve human judgement which may result in substantial error. This report presents a new technique applied to the measurements of nuclei concentration and size distribution in a liquid. This report describes the technique and required instrumentation as well as its application to the cavitation tunnel water in this laboratory. The technique provides statistically valid size spectra for the entrained gas nuclei, and their dependence on pressurization history.

II. OBJECTIVES OF THE REPORT

This report deals mainly with the explanation of the equipment and instruments used in this new technique. The test section which is a part of a water tunnel test facility with venturis and the conventional measuring hydrodynamic equipment is one part and the electronic apparatus with the Coulter-Counter constitutes the main instruments which are the subject of the present study shown in the demonstration.

A. The Water Tunnel Test Facility

This facility includes 4 closed loops in parallel, each equipped with a cavitating test venturi. However, any of the loops can be easily closed off if this is desired. The facility also includes a cold water deaerator and ion-exchange column. Fig. 1 is a schematic of the facility and Fig. 2, a photograph. The main centrifugal pump is driven

by a variable speed prime mover with a range of 900 rpm to 3600 rpm.

In this work two test venturi loops were run in parallel. One of the two venturis comprise the main test section. The use of the other is explained later. It is a cylindrical plexiglas venturi with nominal 3/4" throat diameter and 6° included diffuser and nozzle angle. The cylindrical throat has a length to diameter ratio of approximately 4. To obtain later cavitation damage and pressure pulse measurements, there are three walltaps around the same circumference at about 1.2 inches from the throat exit (Fig. 3). These openings should not interfere with the flow region upstream of this point.

For the nuclei spectrum measurements, a continuous water sampling bypass stream is drawn from a tap just upstream of the venturi inlet. The same tap is also used for measuring the inlet pressure to the venturi. This sampling line is actually a path parallel to the venturi. Bypass flow is approximately 0.2 GPM to insure a good representation of the main stream (100 GPM). The sampling flow is divided into two parts. One is for the nuclei spectrum measurements through the "sampling beaker" at the desired flow rate, from where it is recirculated back to the main venturi outlet. The remainder of the bypass flow is recirculated back to a low pressure point in the loop (Fig. 4). This arrangement is provided because it is not possible to circulate the full bypass stream through the sample beaker, but such a large stream is desired to obtain good sampling of the main flow. In the actual tests, samples are taken at both cavitating and non-cavitating conditions at different pressures and total air contents (measured by "Van Slyke").

In the cavitating conditions, assuming smooth and accurately machined venturi walls, cavitation will be mainly affected by the geometry, the dimensions, the pressure and the velocity of the flow through the venturi throat, and the nuclei spectrum.

However, in order to correlate cavitation number measurements from this venturi with other parameters, it will be necessary to know the time-mean wall static pressures and the minimum wall pressure. For this reason and in order not to disturb the flow in the test section and trigger cavitation prematurely, a second, geometrically similar, venturi, but with pressure taps located axially along the venturi walls is used. Of course, these taps, specifically those ones upstream and near the throat exit may create minor dissimilarity between the flows in the two venturis, it is believed that these are very small and may be neglected. Thus, it is reasonable to assume that the pressure profiles measured in the second venturi represent closely those that in the first one, provided that the inlet and exit pressures of both venturis are equal.

B. Water Sampling Technique

The water for sampling is taken, as previously stated, from a position near the venturi inlet, and hence through a 3/4" diameter plastic tube. The sampling probe in the loop itself is located near the center line of the main pipe through a tapered tip tube parallel to the flow. The total bypass flow is measured by a rotometer (0 - 1.5 GPM). The sampling flow is then divided into three parallel branches, two are continuously open and the flow in the third is intermitent. The first branch represents a continuous return flow to a low pressure region of the main loop. It is used to bring a reasonably continuous sampling stream quickly to the vicinity of the sample beaker, since it is not physically possible to locate the sample beaker closer to the primary flow. The second continuous flow branch leads to the sample beaker itself. Physically, this makes the sample beaker about 18 inches from the main sampling line. The flow through this branch is about 0.1 GPM. A small part of this (about 2.5 cc/min) is monitored by the Coulter

Counter for nuclei content, the rest returns to the loop. The intermittent branch (Fig. 3) is mainly for filling the Coulter-Counter tube and for flushing it before each measurement to insure that equalization of temperature inside and outside the measuring tube. This is necessary to reduce the error due to electrical resistance change of the water as a function of temperature. The level in the beaker required such that the outside platinum electrode of the Counter be completely covered by the water. The sample flow through the beaker and the level in it are controlled by two valves, one is the branch that comes from the loop and the other is on the line to the main venturi discharge. Once the flow and the level are adjusted the sampling flow rate should remain stable. However, due to small fluctuations in the air pressure the operator must observe and correct any changes in the level.

C. The Pressure Chamber

In order to modify the Coulter Counter so that it could be used to measure the nuclei spectrum as it exists at the inlet of the venturi, a pressure chamber constructed of a 12" diameter plexiglas cylinder with 1/4" thick wall and two aluminum end plates has been developed which entirely encloses the Coulter Counter (Fig. 5).

Through the lower plate, there are the following inlets and outlets:

1. Water inlet to the sample beaker
2. Water inlet to the Coulter tube
3. Water outlet to the main venturi downstream tap
4. Water drain for the measured specimen and the filling and flushing of the Coulter tube from the collecting flask
5. High pressure shop air inlet to the chamber
6. Low pressure shop air inlet to the collecting flask
7. Two pressure taps: one for the pressure chamber and one for the collecting flask to the differential mercury manometer

8. Electrical connections

9. Over flow drain

The cylinder is covered by a grounded metallic mesh wire for electronic shielding.

D. The Coulter Tube

The Coulter tube shown (Fig. 6) is a precise blown-glass tube with a very precise sapphire orifice fused into its lower end wall. Orifices of different sizes (30 micron to 500 micron dia.) can be used. The choice of orifice diameter depends on the diameter of particles to be measured. For best results and minimum error the minimum orifice diameter should be 4-5 x the biggest particle diameter to be detected. The error in estimating the true size of a particle greater than these limits will vary between 5% to 10%.

In this study three orifice sizes were tried, since the nuclei size spectrum was unknown. A 50 micron dia. orifice tube was first used. However, beside its inconveniently low flow rate, it was very subject to clogging by unknown particles (probably solids, not necessary single ones). A 100 and a 150 micron orifice tube have since been tested. Particles of diameters as large as 20 microns have been detected. Consequently, the 100 μ orifice tube was selected for all the tests.

When this tube is immersed in the sample beaker it forms an electric cell, together with the two platinum electrodes, one inside the tube and one outside of it, immersed in the sample beaker. The liquid connection through the orifice is then the only electric current-carrying medium. As mentioned before, the tube is filled and flushed through a tube inside it, which reaches to about 1/2 inch above the orifice. The water specimen being tested flows through the orifice as a result of the pressure difference between the beaker sample and the pressure inside the tube. After the test, the measured sample is drained to the collecting flask.

E. Theory of Operation of the Coulter Counter

The basic assumption underlying the operation of the Coulter Counter is that the voltage pulse generated when a particle passes through the orifice is directly proportional to particle volume. The reliability of the instrument depends upon the accuracy of this assumption.

The relationship between response and particle size may be determined in the following manner. Fig. 7-a shows a particle passing through the orifice and Fig. 7-b shows an element of the particle and orifice. The resistance of the element of orifice without a particle can be given by:

$$\delta R_o = \frac{\rho_p \delta l}{A}$$

The resistance of the element with a particle included is that of two resistance in parallel

$$\frac{1}{\delta R} = \frac{1}{\frac{\rho_f \delta l}{A-a}} + \frac{1}{\frac{\rho_p \delta l}{a}}$$

or

$$\delta R = \frac{1}{\left[\frac{A-a}{\rho_f \delta l} + \frac{a}{\rho_p \delta l} \right]}$$

ρ_f and ρ_p are the resistivities of the fluid and the particle, respectively.

Thus the change in the resistance of the element due to the presence of the particle is given by:

$$\Delta R = \delta R_o - \delta R = - \frac{\rho_f a \delta l}{A^2} \left(1 - \frac{\rho_f}{\rho_p} \right) \frac{1}{1 - \left(1 - \frac{\rho_f}{\rho_p} \right) \frac{a}{A}}$$

The external resistance in the circuit is sufficiently high to ensure that the small change ΔR in the resistance of the orifice due to the presence of a particle will not significantly affect the current I , in the circuit; the voltage pulse generated is therefore $I\Delta R$. In practice, it is found that the response is independent of the resistivity of the particle. In fact, if this were not so, the whole technique would break down, since a different calibration factor would be required for each electrolyte-solid suspension. Berg⁽¹⁾ suggests that this may be due to oxide surface films on solid particles or ionic inertia of the Helmholtz electrical double layer, and associated solvent molecules at the surface of the particles, their electrical resistivity becoming infinite. The terms involving ρ_f / ρ_p may therefore be neglected. Thus the above equation becomes

$$\Delta R = \frac{\frac{\rho_f a \delta l}{A^2}}{\left(1 - \frac{a}{A}\right)}$$

The response therefore is not proportional to the volume of the particle but is modified due to the term a/A . The magnitude of the error involved in this simplification may be determined for a spherical particle of radius b totally enclosed within the orifice as follows.⁽²⁾

From Fig. 7-a, if the distance of the element from the center of the sphere is l ,

$$\Delta R = - \frac{2 \rho_f \pi}{A^2} \int_0^b \frac{(b^2 - l^2)}{1 - \frac{\pi(b^2 - l^2)}{A}} dl$$

$$= - \frac{4}{3} \pi b^3 \cdot \frac{\rho_f}{A^2} \left[1 + \frac{4}{5} \frac{\pi b^2}{A} + \frac{24}{35} \frac{\pi^2 b^4}{A^2} + \dots \right]$$

Since $A = \pi D^2/4$ where D is the diameter of the orifice and it is advisable to keep $2b/D$ smaller than 0.4, the maximum error due to the modifying terms is +14.6%. Thus the use of the simplified formula leads to a maximum error of approximately 5% in the measured diameter of the particle. With a 100 micron orifice, a 38.2 micron

diameter particle will be measured as 40.0 microns, a 28.6 micron as 30 microns, 19.7 micron particle as 20 microns and so on. The errors being 4.8, 2.8 and 1.7% respectively. Particles of this last diameter, (rag weed particles) were used for the purpose of calibration in this work. With "rod-shaped particles" it can be shown that the maximum error corresponding to 4.8% error for spheres is 6%.⁽²⁾ Hence the instrument consistently "reads high", the error becoming appreciable as the particle size approaches its upper limiting value.

Using the 100 micron tube the maximum diameter of particles detected in this study is about 20 microns; the error is negligible.

F. Electronic Instruments

Fig. 8 is a block diagram of the instruments used in this work, and Fig. 9 is a photograph of the set-up. Their description and function are given below.

1. Pulse Generator:

To check the linearity of the amplifier, pulse shape and multi-channel pulse height analyzer, the Coulter tube input was replaced by the input of a Radiation Instrument Development Laboratory, mercury pulse generator, model 47-1 serial no. 60, which generates pulses of uniform height and shape. The desired pulse amplitude, duration and rise time can be selected. There are three amplitude ranges: 0-1 volts, 1-10 volts and 1-100 volts with positive or negative polarities. There are four ranges of pulse duration: 1, 2, 10 and 100 μ seconds. The rise time has a continuously variable range from 0.5 μ seconds to 2 μ seconds.

Since the purpose of the pulse generator is to check only the linearity of the above mentioned instruments, the selection between these ranges was arbitrary, but within the limitations of instruments, specifically the pulse shaper.

2. Amplifier:

A custom-built amplifier was used which was designed to suit the required measurements and for use with the other equipment. It serves as a power supply to the cell of the Coulter tube and as an amplifier which can retain the shape of the input at a very low noise to signal ratio. However, the amplifier is not precisely linear at its very low gain ranges.

3. Interface pulse shaper:

Because of the physical construction of the safire orifice, the time of the input pulse ranges between 5 \rightarrow 50 μ seconds depending on the size of the particle and the rate of flow through the orifice. Since the amplifier will retain quite closely the same pulse shape, these pulses will not be suitable for pulse height analysis, since the analyzer can accept only pulses of 0.5 μ seconds to 3 μ seconds for optimum performance. It was thus found that pulse-shaping was necessary to retain the proportionality between amplitude and nuclei size while rise time and duration must be reduced to the range required by the analyzer.

To fulfil this necessity, a solid state pulse shaper was designed and built to suit these requirements. Although the pulse shaper is linear, its linear output range is limited to 0.5 \rightarrow 9 volts by unavoidable limitations in the design. Outside this range, linearity ceases. The amplitude of the output pulse will be directly proportional to the amplitude pulse, but has a standard rise time of 0.5 μ seconds and duration of 3-4 μ seconds. The pulse shaper has also its built-in count rate meter which can be connected to a scaler, either to give the total count rate, i. e., the nuclei count rate, or the number of pulses above a certain amplitude, by using a triggering level. The shape of the pulse is shown in Fig. 10 and the circuit diagram is shown in Fig. 11.

4. The Multichannel Analyzer :

The multichannel analyzer is basically an instrument that can analyze certain shapes of pulses according to their amplitudes. It has

a wide popularity in the field of nuclear radiation. The analyzer used for this work is an ND-110, 128 channel analyzer shown in Fig. 12. The data can be derived in either two ways: a) by analyzing the signal on an amplitude basis or b) by analyzing the signal on a time basis. For all the measurements done here the analyzer was used on the first basis. Such amplitude analyses of signal pulses determine the distribution of nuclei sizes as related to the amplitude of the input pulse from the pulse shaper. During a measurement, incoming pulses are analyzed by the ND-110 and the resulting data is stored in its magnetic core ("memory"). Data stored in the memory can be observed in an analog form, either during or after accumulation, on a cathod ray tube of any ancillary oscilloscope (Fig. 13). This visible presentation aids in establishing control settings and enables the operator to monitor the progress of the measurements. Afterwards, the accumulative stored data is read out in digital or analog form for permanent record. The read-out is by an IBM selectric typewriter.

There are only a few general types of signals which can be accepted for pulse height analysis. One of them is the positive signal from a transistorized amplifier with a range of 10 volts which is the case with the pulse shaper in this work. For the highest resolution and linearity the input signals should have an exponential rise with a rise time of $0.25 \rightarrow 0.75 \mu$ seconds and a duration not more than 3 to 4μ seconds with a "flat top" of a minimum 3 to $4/10$ th's of a μ second at the maximum voltage value. These requirements determined the design of the pulse shaper.

G. Calibrations

1. Checking the linearity of the pulse shaper:

A constant input from the pulse generator was fed through the amplifier to the pulse shaper. The reason for not using the pulse generator directly is to insure that the amplifier input impedance will

be taken into consideration during the calibration. The gain of the amplifier was varied over the possible range which is suitable to the pulse shaper input. The amplifier gain dial setting was thus varied between 0 \rightarrow 15.

The input pulse to the shaper together with its output were displayed on a dual beam oscilloscope and the calibration was made by using Polaroid scope photographs. The various input and output pulses at various gain settings of the amplifier are shown in Fig. 14. The output was plotted against the input, and the relation shown to be linear, although not with a 45° slope (Fig. 15). The results are linear only within the input voltage range of 0.5 volts to 10 volts, corresponding to an output range of 0.5 volts to 8.5 volts. The previous discussion of the multichannel analyzer and the following discussion on the Coulter Counter calibrations will show that these results will fulfil the requirements of the measurements.

2. Checking the Linearity of the Multichannel Analyzer:

The output of the pulse shaper was fed to the multichannel analyzer at the +10 volts input jack. The pulse amplitude was varied in steps and the analyzer was set to analyze each input. Since the input pulses at one setting are of the same amplitude, they will be accumulated in one specific channel corresponding to that amplitude. The final analyses of the various input pulses were given in digital form by the IBM typewriter, while the amplitudes of the input pulses were also measured by taking polaroid photographs from the monitoring scope. The channel numbers corresponding to each input amplitude were plotted and are shown in Fig. 16. The relation between the size of the pulse and the channel number was proved to be linear. The relation is useful in calibrating the analyzer in such a way as to read the output directly in absolute units of size, as will be shown below.

3. Calibration of the Coulter Counter Together with Related Apparatus:

In order to calibrate the Coulter Counter as well as the whole measuring arrangement so that the output would be the size distribution of particles in absolute size units, standard size particles were used. The Coulter Counter measures directly the volume of particles. Preliminary investigations showed that nuclei in the loop water range from $\sim 4\mu$ to $\sim 20\mu$ in diameter, (i.e., volume range of $34 \mu^3$ to about $4000 \mu^3$). Thus, two different size standard particles were used to cover this wide range. Latex particles of diameter between 6 and 14μ (most probable diameter of 10 microns) were used to cover the small size nuclei range, using gain setting between 5 to 15 on the amplifier dial. For gains below 5, the results were not satisfactory because of the increased noise to signal ratio, since the output pulses were small.

To cover this lower gain range, larger particles were used. Ragweed pollen particles of most probable diameter of 19.5μ , i.e., about $3880 \mu^3$, were used. The maximum gain setting for these particles is 2, otherwise the peak will be off the analyzer scale. For these calibrations, the low pressure inlet of the pressure chamber was connected to a vacuum pump, while the high pressure inlet was opened to the atmospheric pressure.

The particles were prepared as a suspension in water, and one or two drops of this suspension mixed with the water from the loop in the sample beaker. The size spectrum of these particles were obtained for different gain settings of the amplifier in the above mentioned ranges.

The resulting spectra are shown in Fig. 17 for the ragweed pollen at gain settings of 0.5, 1.0, 1.5 and 2. The spectra for the latex particles are given for gain settings of 3.5, 5, 7.5, 10, and 12.5 in Fig. 18. For gains less than 3.5, the spectra were confused with the noise signal.

There are two reasons for these calibrations: 1) to obtain an absolute calibration for the whole set up such that the output spectrum will be given on an absolute scale of size units, i. e. , cubic microns, μ^3 ; 2) to correct for the range limitations of the available instruments. The calibration of the size ordinate corresponding to each gain setting can then be avoided, using a calibration curve such as Fig. 19. The curve starts to drop sharply in the low gain range because of the poor linearity of both the amplifier and the pulse shaper in that gain range, it then becomes quite linear from 3.5 gain until limited at the high gain by the nonlinearity of the pulse shaper above gain 15. The lower range of the calibration curve will be used mainly for detecting large size nuclei if they exist, while the rest of the range will be used for most of the measurements.

H. Actual Measurements Demonstrations

To demonstrate the use of the overall system, typical water tunnel runs were made, and measurements of the nuclei spectrum obtained. These results indicate particularly the stability with time of the cavitation nuclei spectra in the water tunnel. The water tunnel was run under constant pressure, velocity and air content for a 24 hour period, and the nuclei spectrum were measured at different intervals.

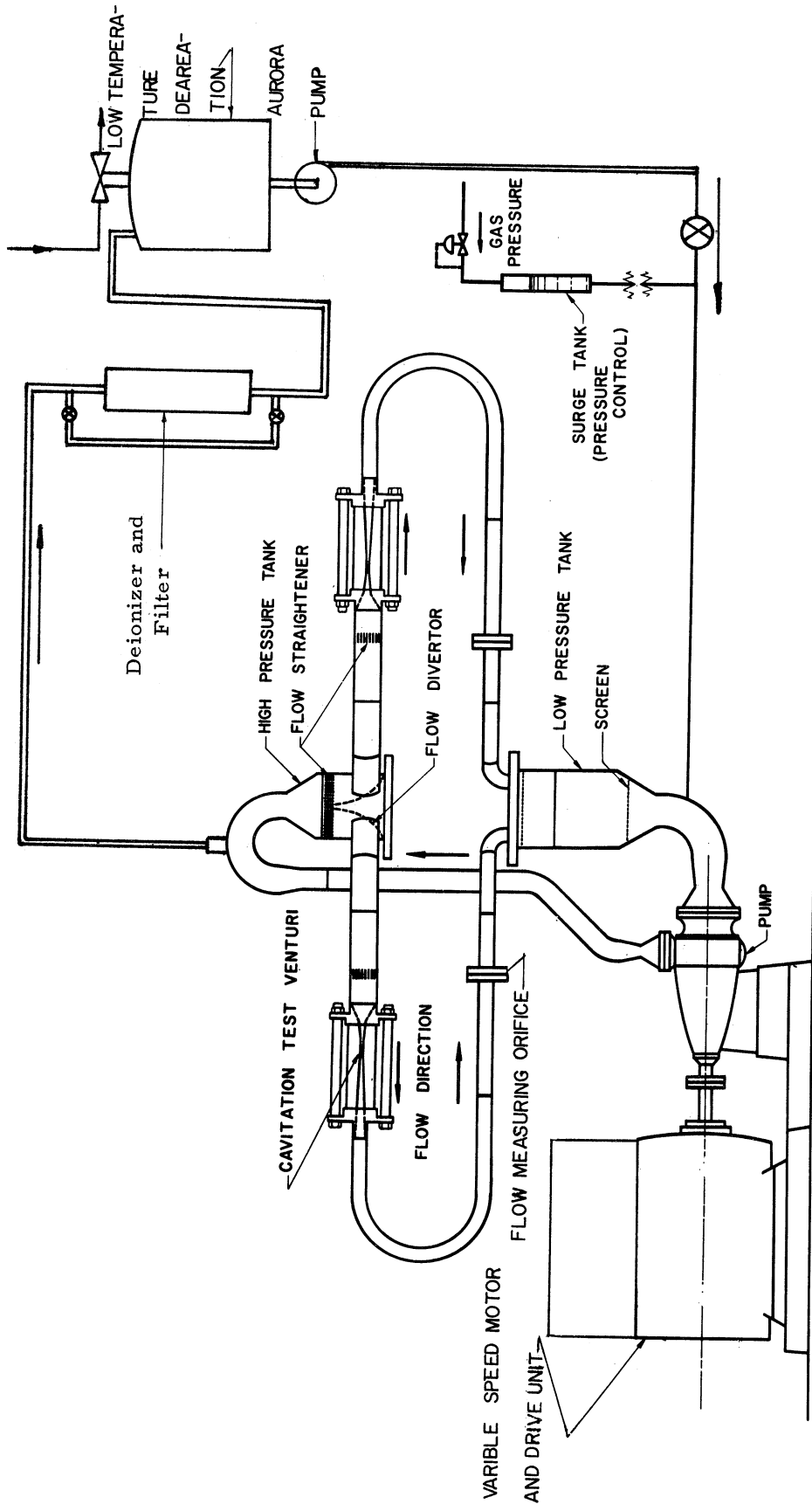
The preparation of the tunnel and the pressure chamber for the measurements, i. e. , adjusting the pressure, the velocity and the flow rate, required about 30 minutes. The end of this initial 30 minute period was considered the zero time for taking the measurements, and the first measurement was taken at that time. Other measurements were taken at different intervals (Fig. 20). For a statistically good observation, a minimum counting time of 4 minutes was used. With some minor adjustment in the flow rate through the orifice tube, a sample of about 10 cc was processed in the counting time. The sample

volume was measured in a calibrated cylinder. The sample flow rates for the various runs varied between 9.4 cc/min to 10.5 cc/min. This variation was mainly due to an unavoidable fluctuation in the air pressure to the chamber. However, the average collected sample for the 16 runs was about 9.9 cc/4 minutes.

Fig. 20 shows that the nuclei content decreases with time. These spectrums are the best fit for the experimental data obtained by using the least square method.

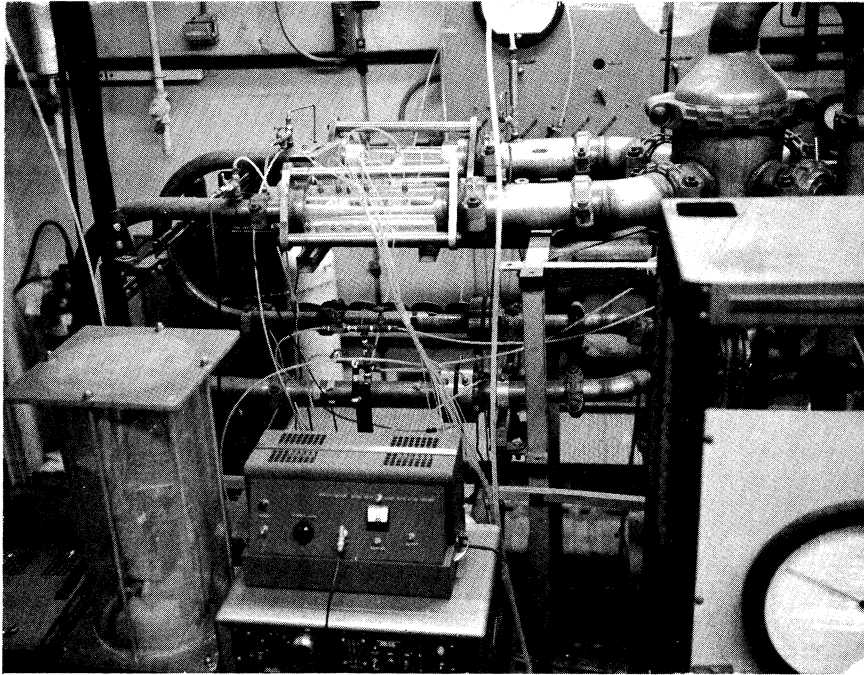
To show the behavior of the spectra with time, the total entrained gas content represented by the area under the curve was plotted against time (Fig. 21). Entrained gas content decreases with time at a moderate rate until it reaches an approximate saturation value after 24 hours.

Further measurements are to be done to study the same effects under cavitating conditions as well as the effect of varying pressure and total air content. In conclusion, the above mentioned technique for cavitation nuclei spectrum measurements appear to be faster and more reliable than other techniques used for the same purpose, such as sound and light attenuation or scattering.



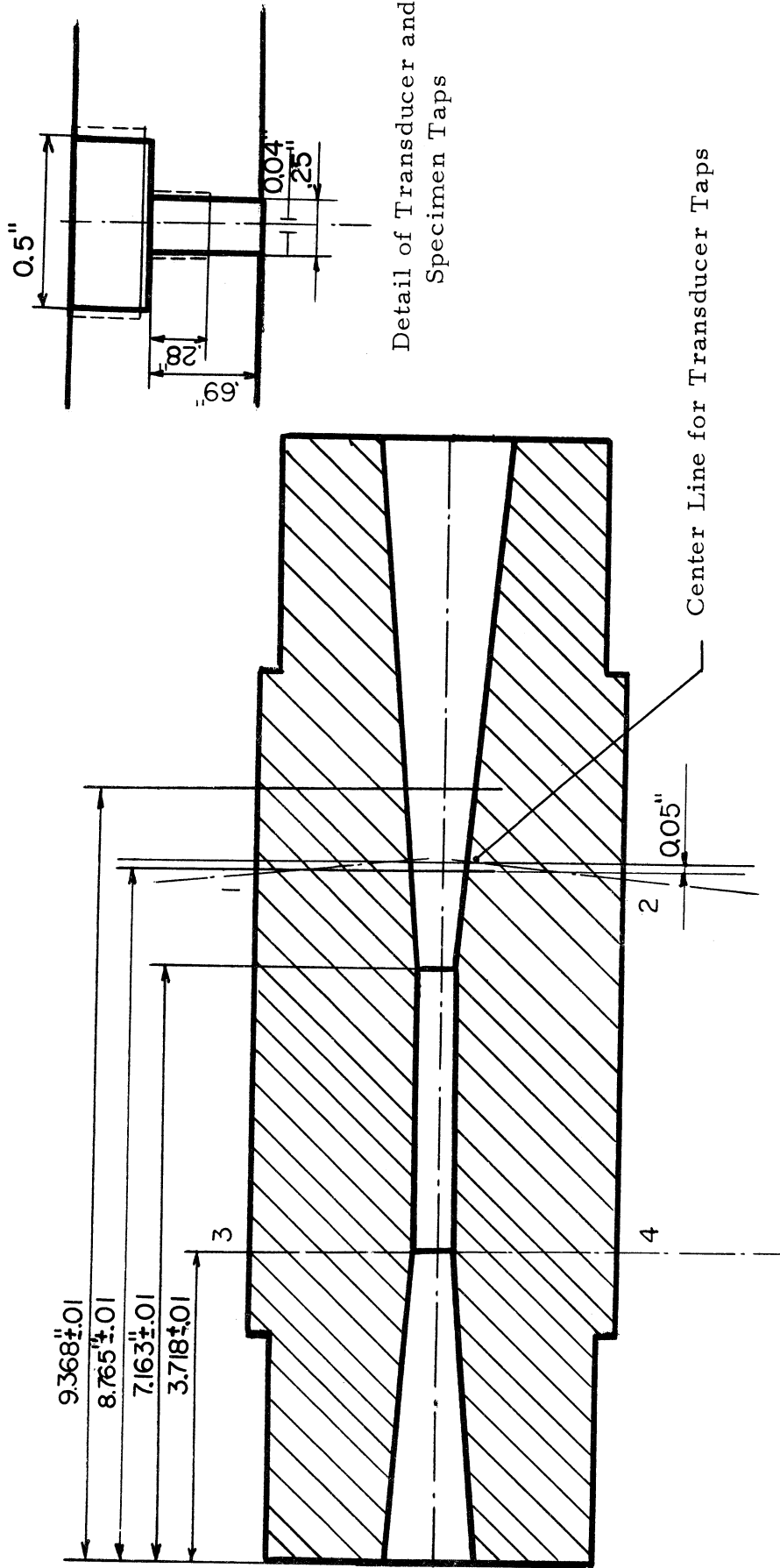
1236

Figure 1. Schematic of Water Tunnel Test Facility



3070

Figure 2. Photograph of Water Tunnel Test Facility



3/4" Plexiglas Venturi with Transducer Taps and Specimen Locations

Figure 3. Venturi Test Section

307I

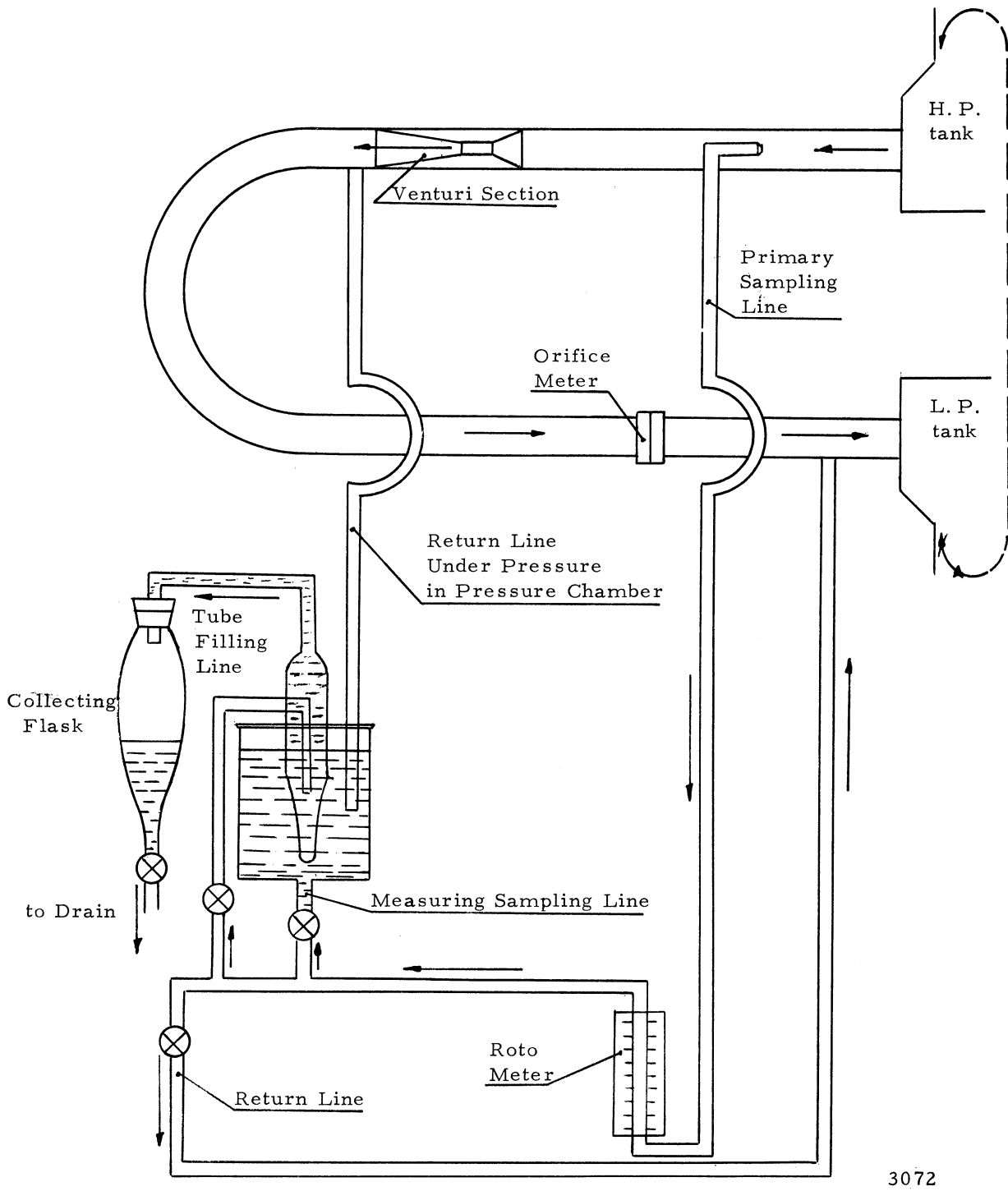
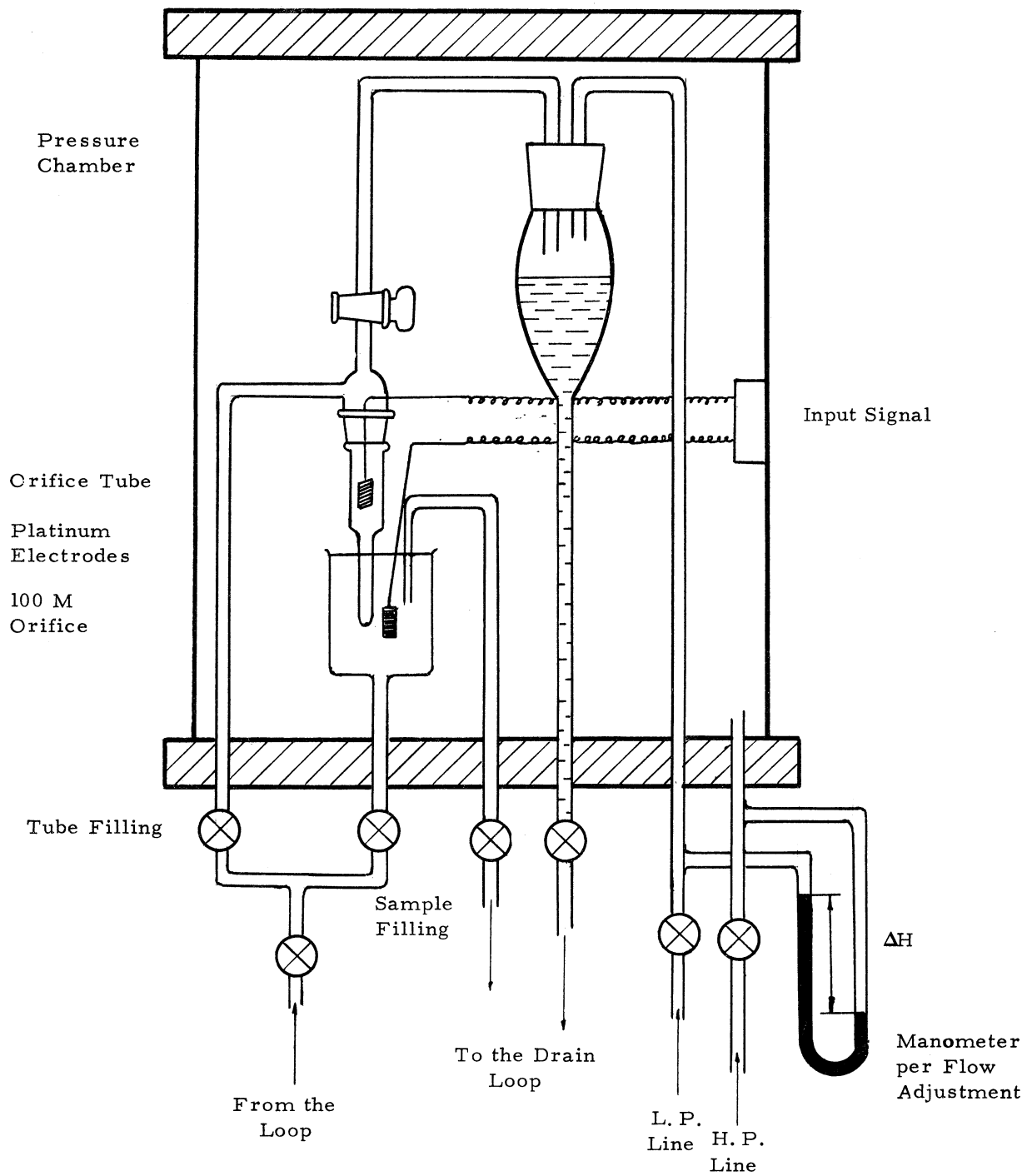


Figure 4, Schematic of Sampling Line



3073

Figure 5. Schematic of Pressure Chamber

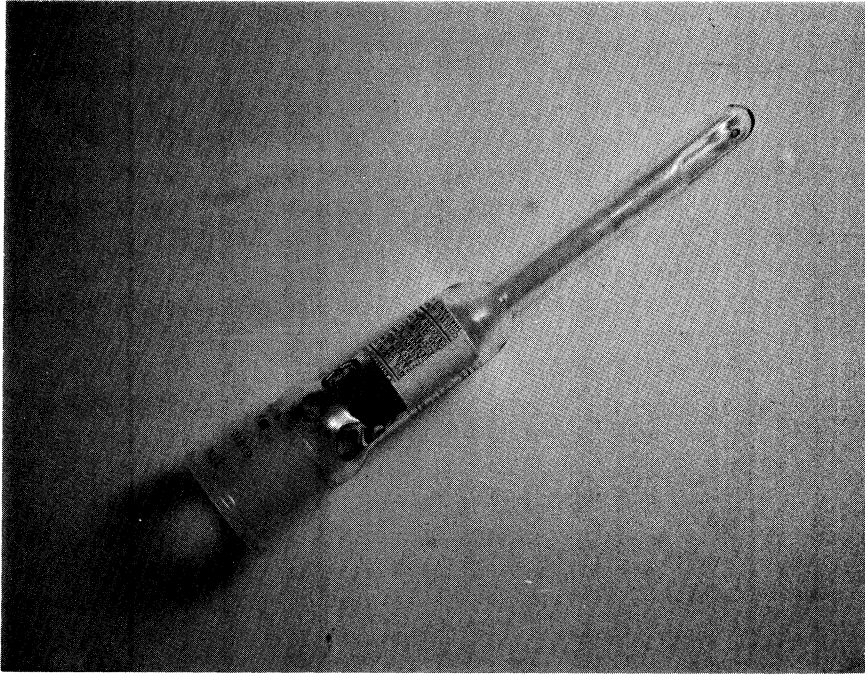
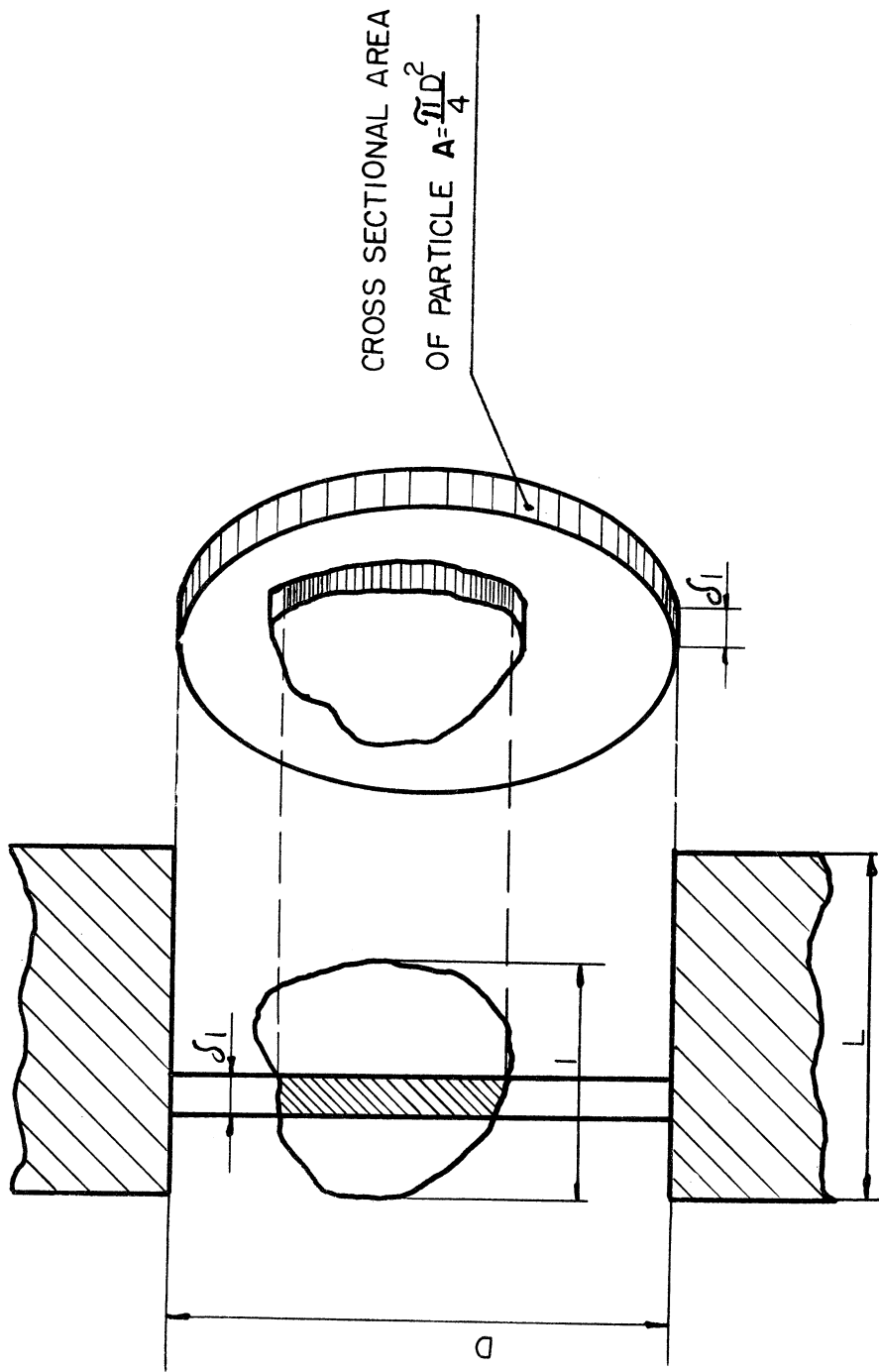


Figure 6. Photograph of Coulter Tube

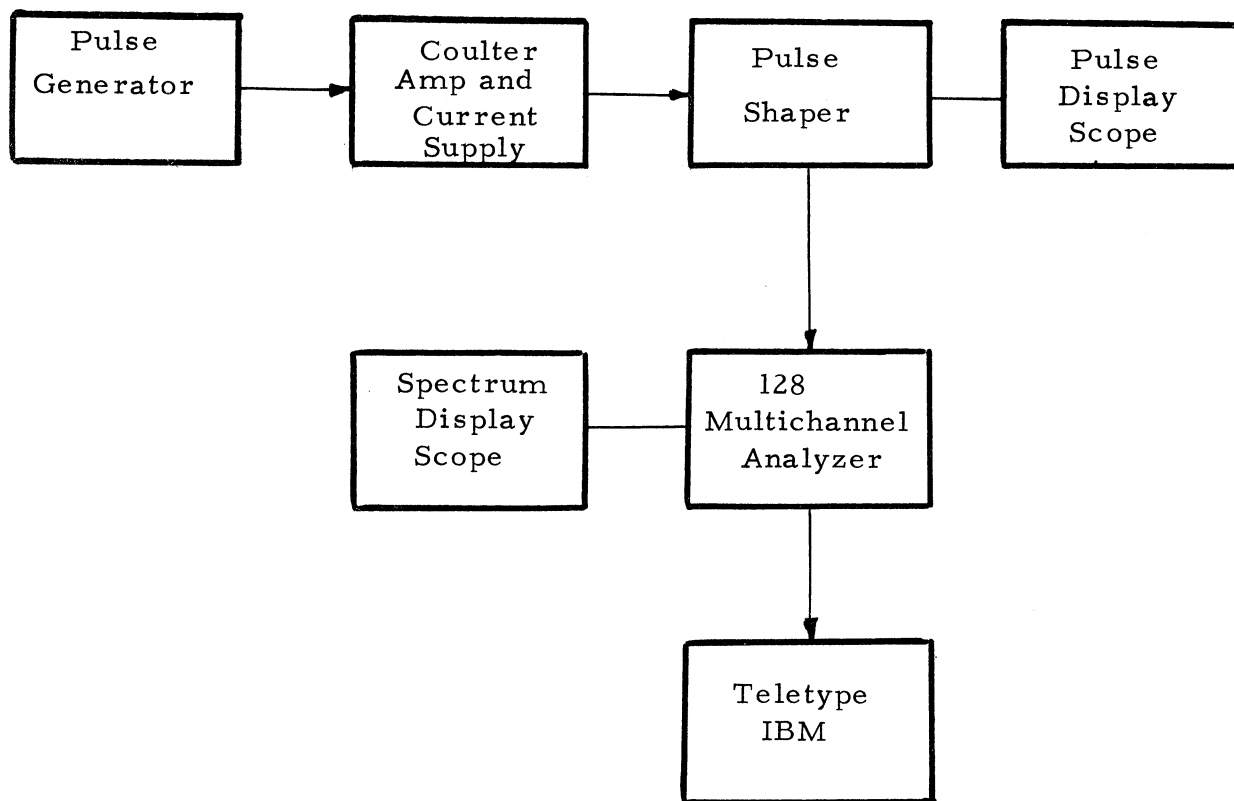


3075

(a) (b)

Figure 7a. Particle Passing Through the Orifice

Figure 7b. Section of an Element of the Orifice with
a Part of the Particle Passing through it



3076

Figure 8. Block Diagram of the Electric Instruments Used in Test

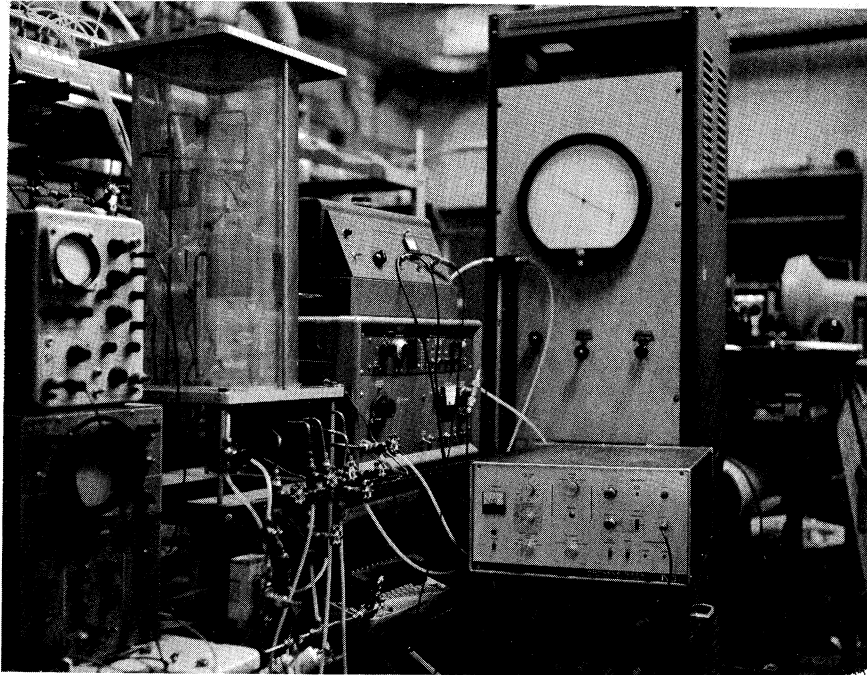
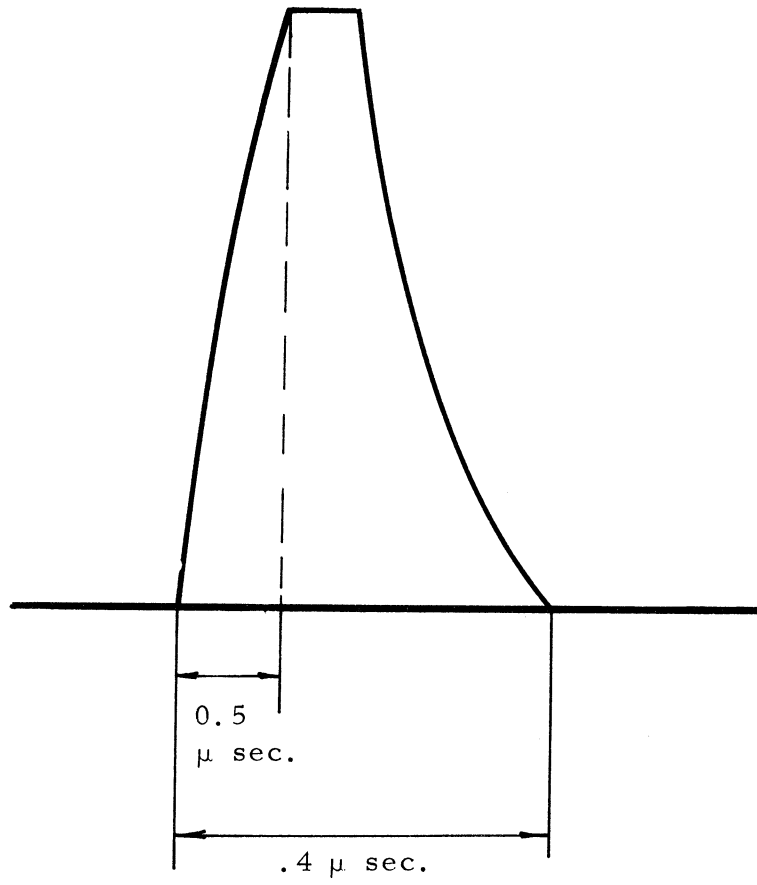


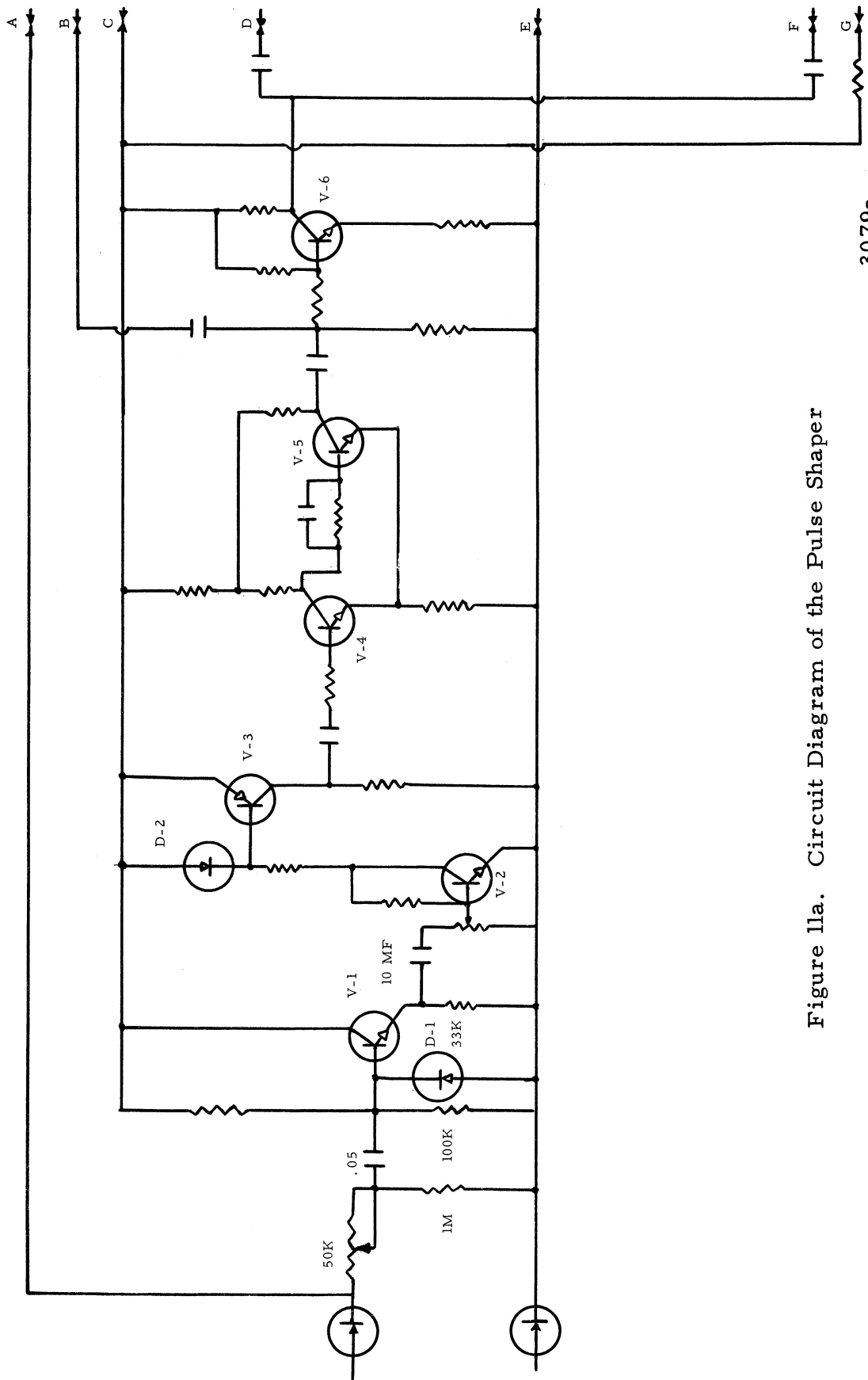
Figure 9. Photograph of Complete Set-Up

3077



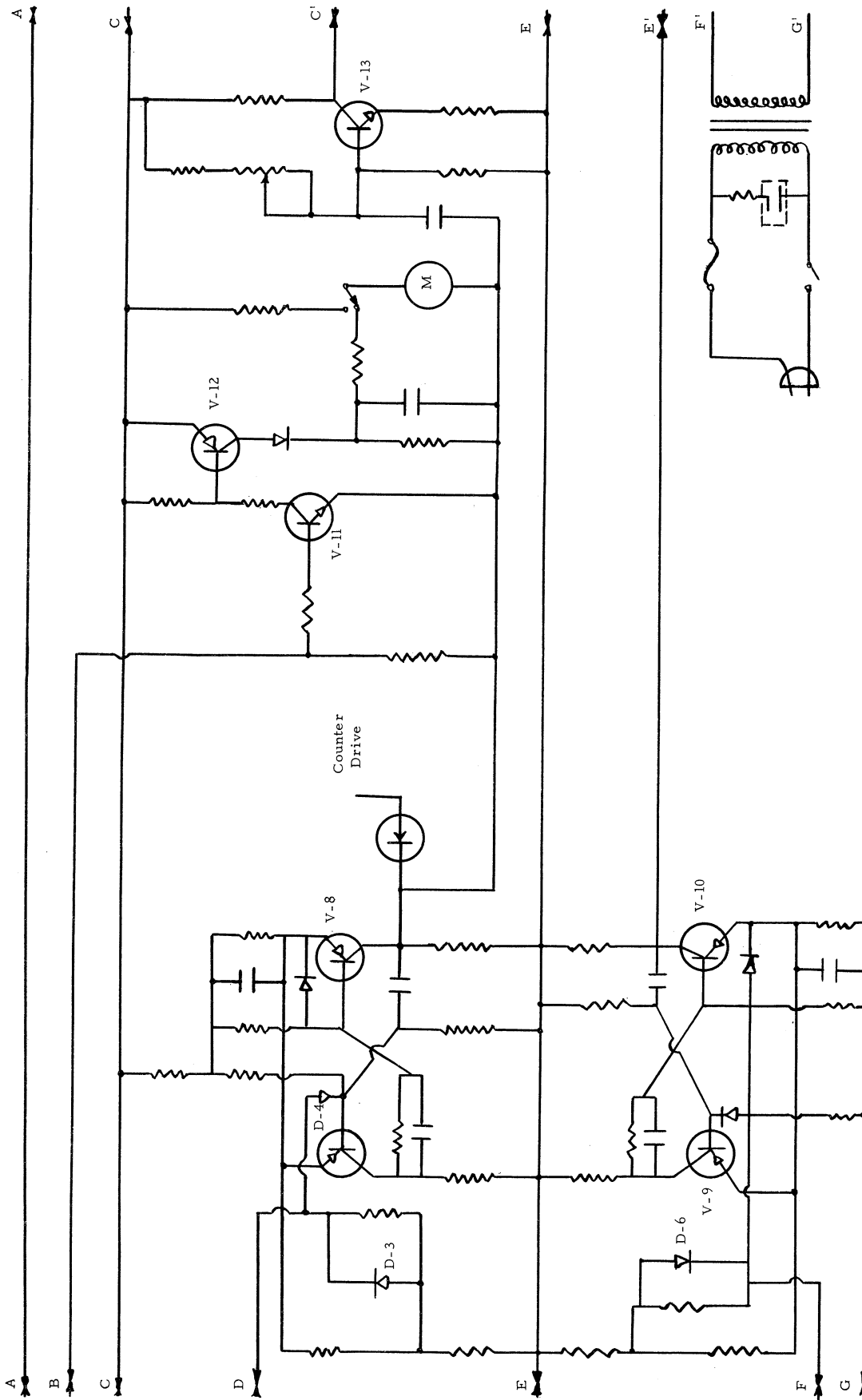
3078

Figure 10. Shape of the Pulse for the Pulse Shaper



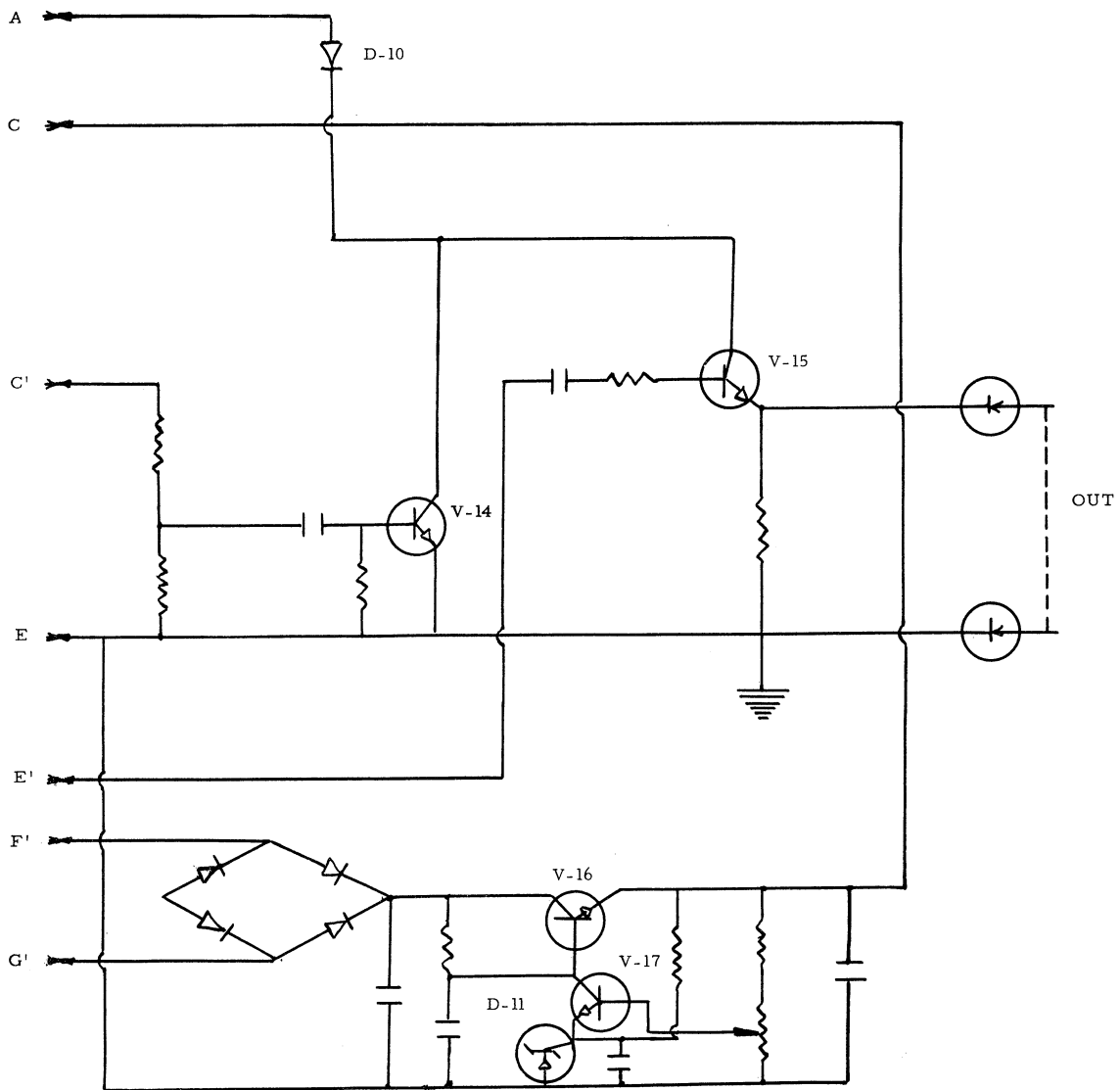
3079a

Figure 11a. Circuit Diagram of the Pulse Shaper



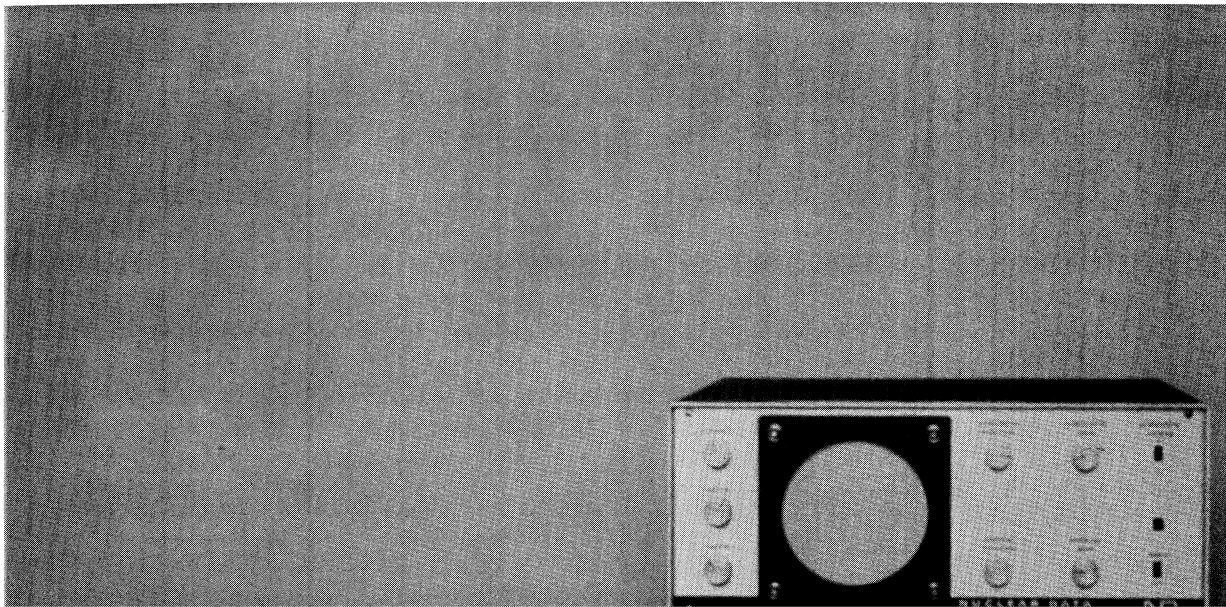
3079b

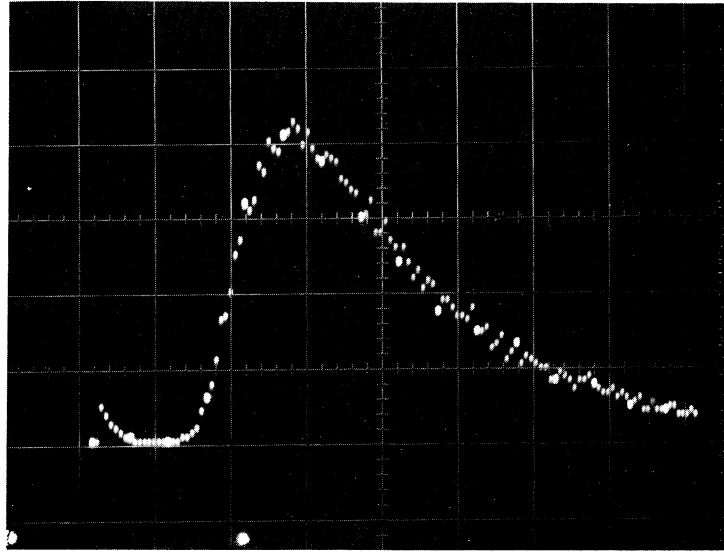
Figure 11b. Continued



3079c

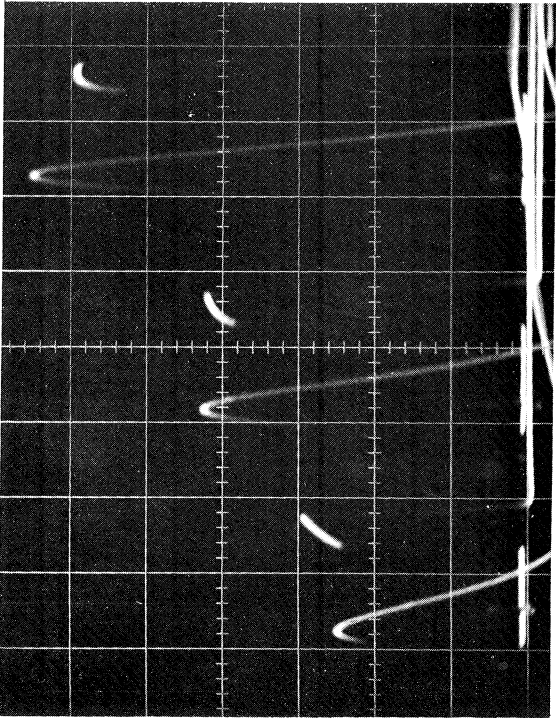
Figure 11c. Continued



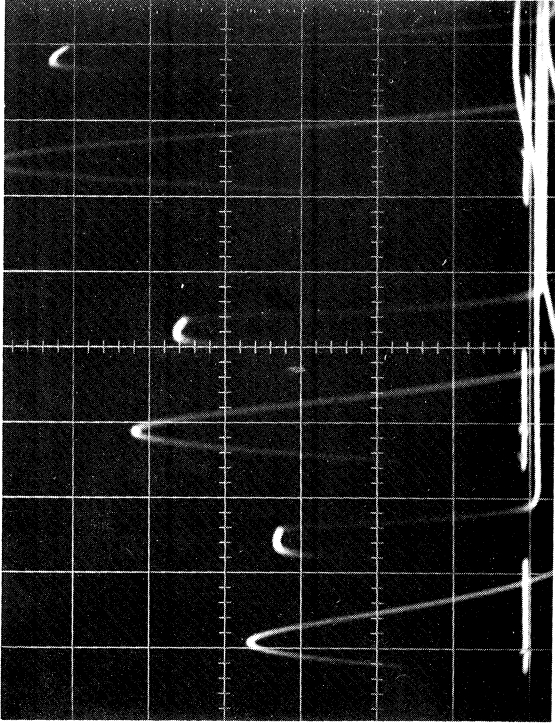


3081

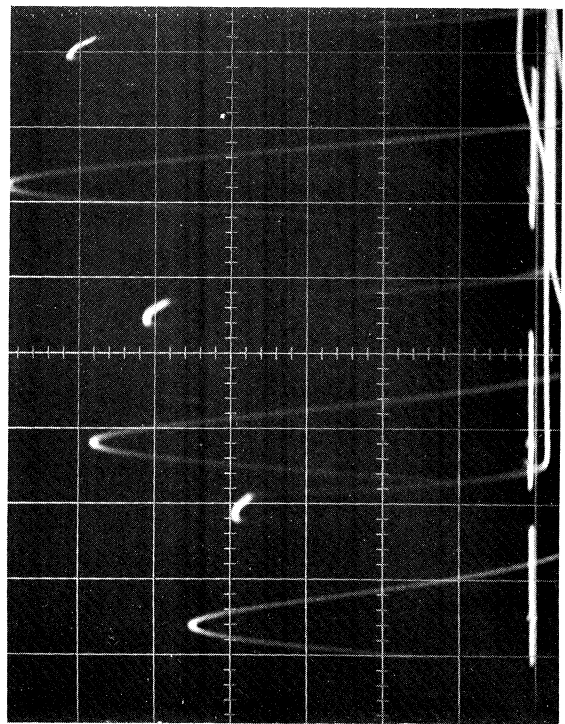
Figure 13. The Form of the Output Spectrum of the Multichannel Analyzer



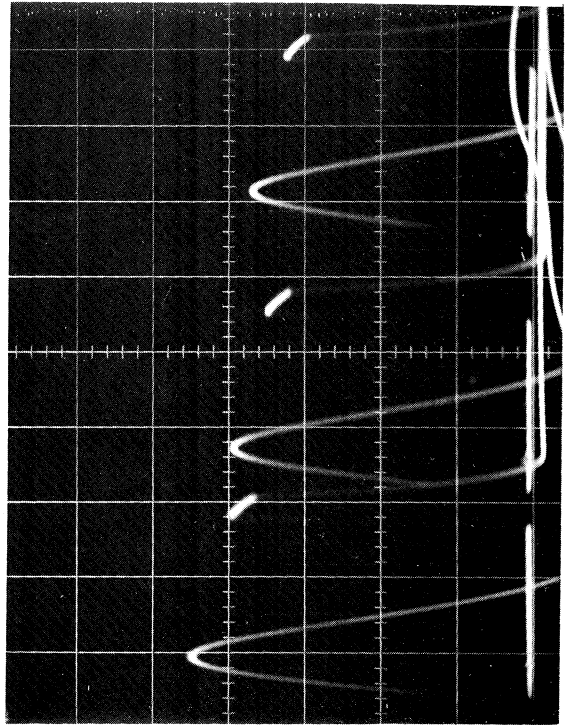
Vertical Scale: 0.2 Volts/cm



0.5 Volts/cm



1 Volt/cm



2 Volts/cm

3082

Figure 14. The Input Pulses to the Pulse Shaper Together

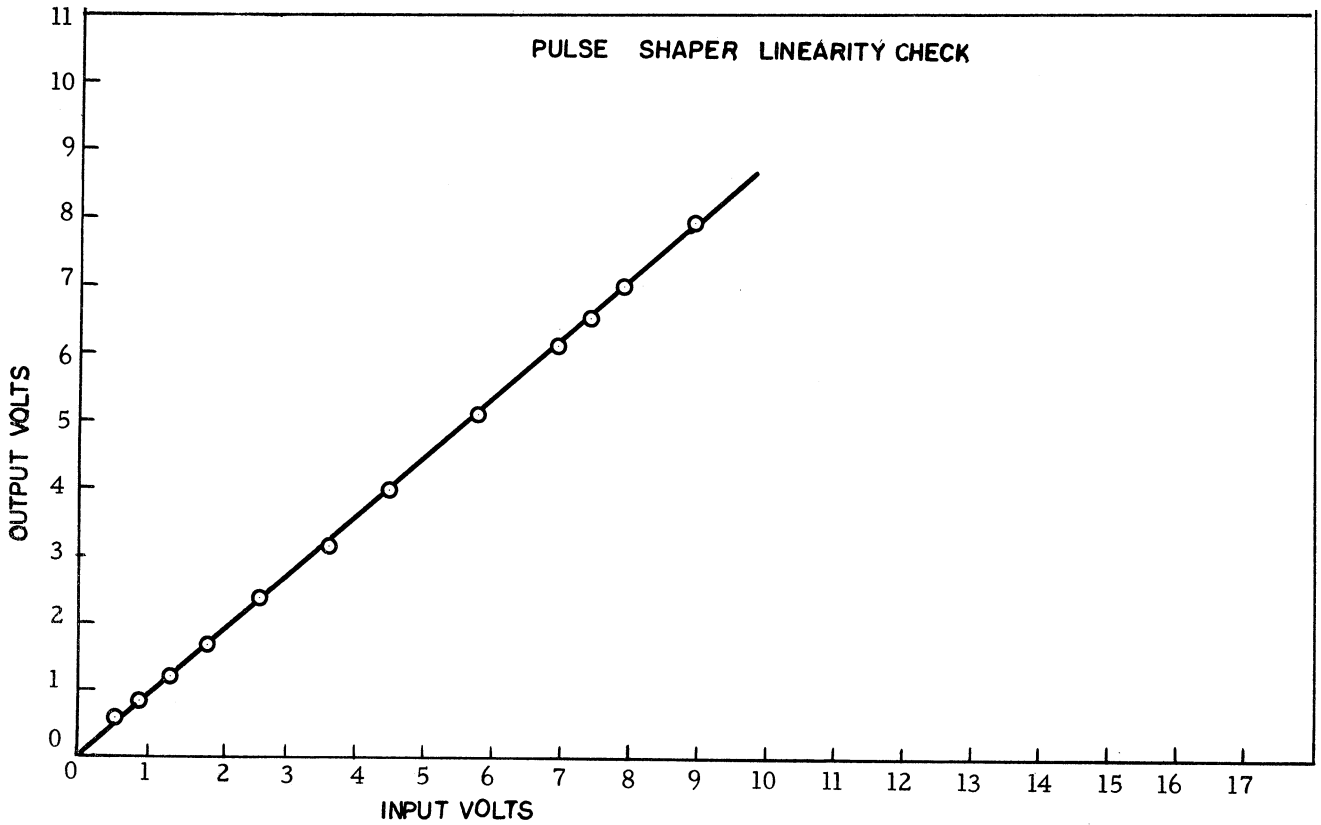


Figure 15. The Linearity Checking Results of the Pulse Shaper

3083

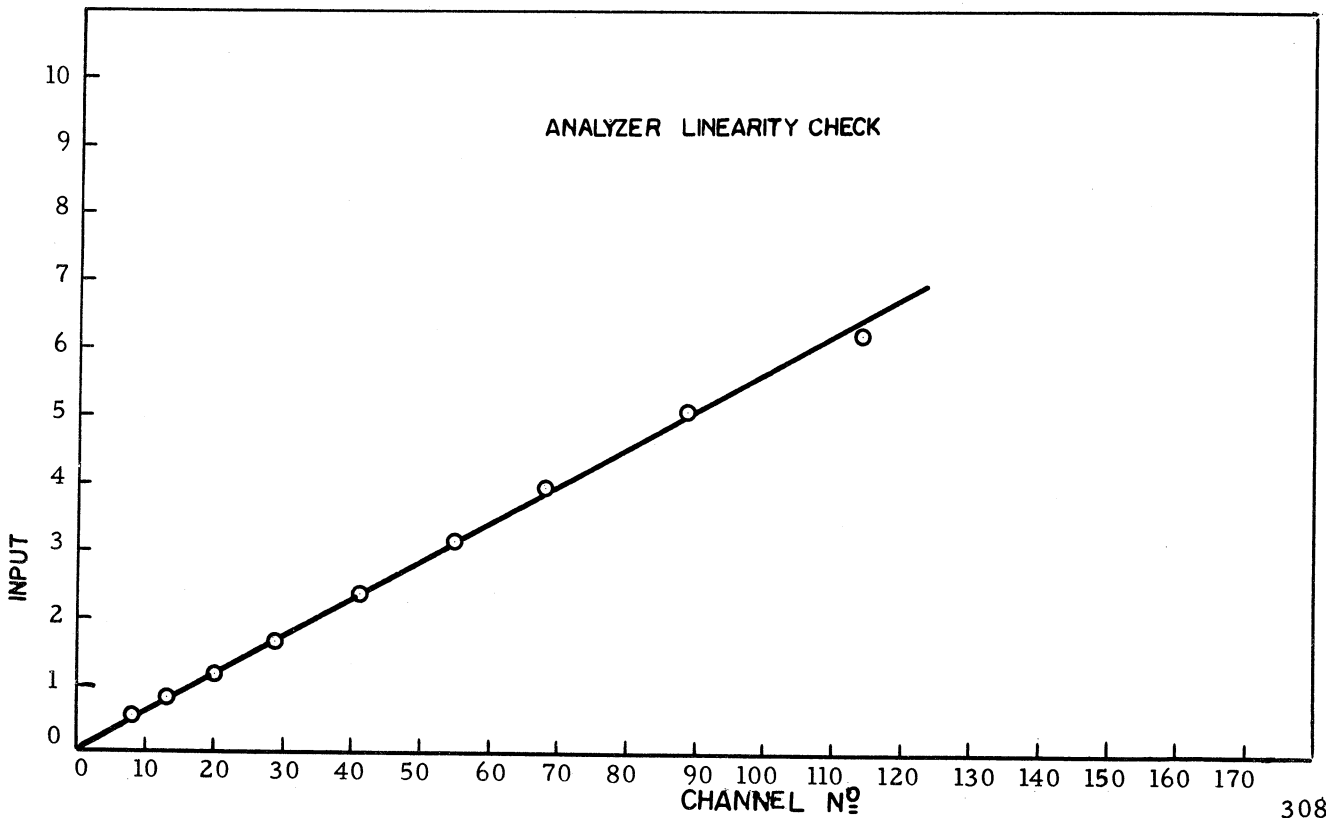
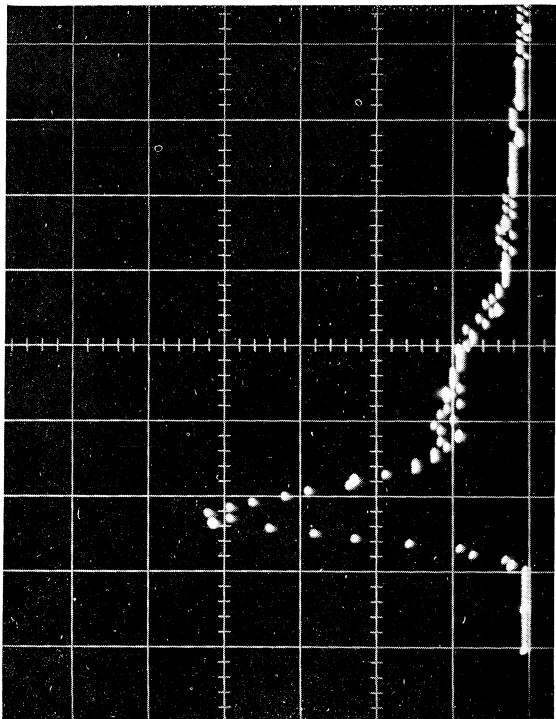
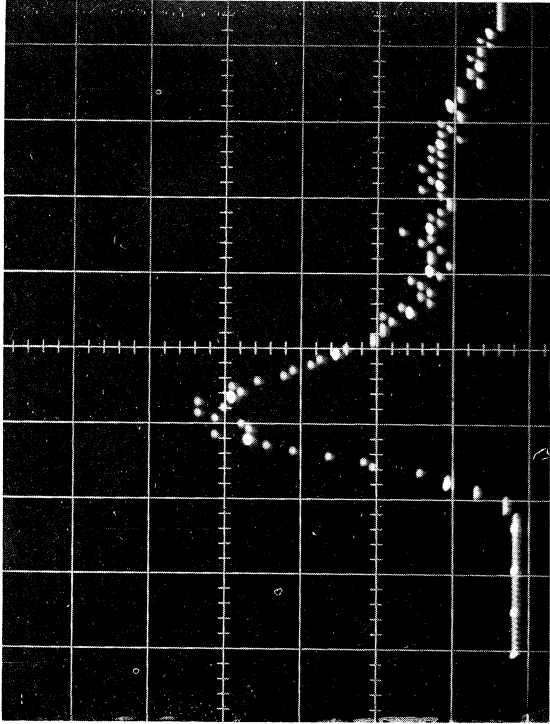


Figure 16. The Linearity Checking Results of the Multi-channel Analyzer

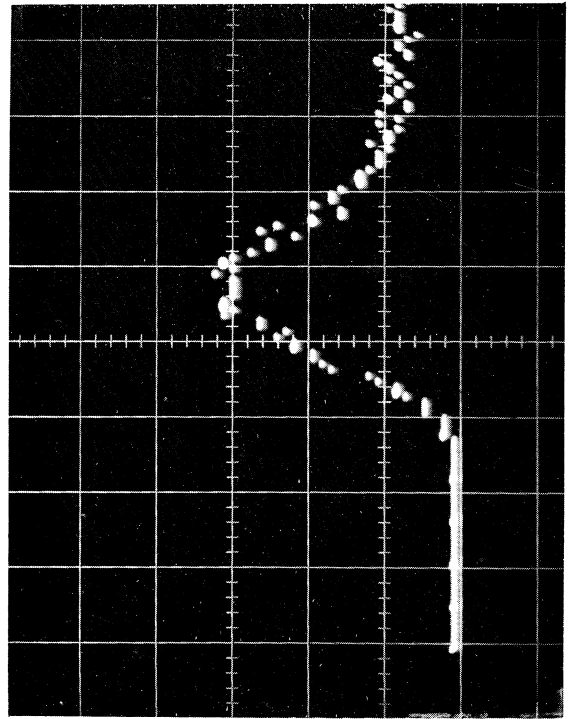
3083



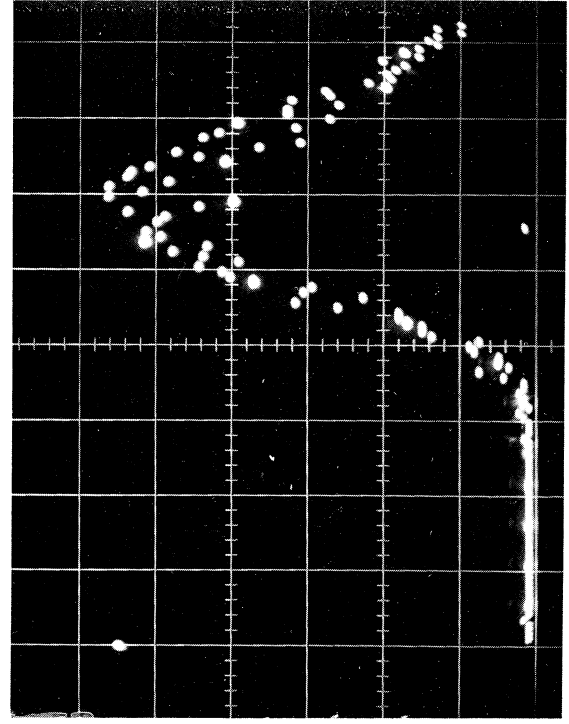
Amplifier Gain Setting: 0.5



1.0



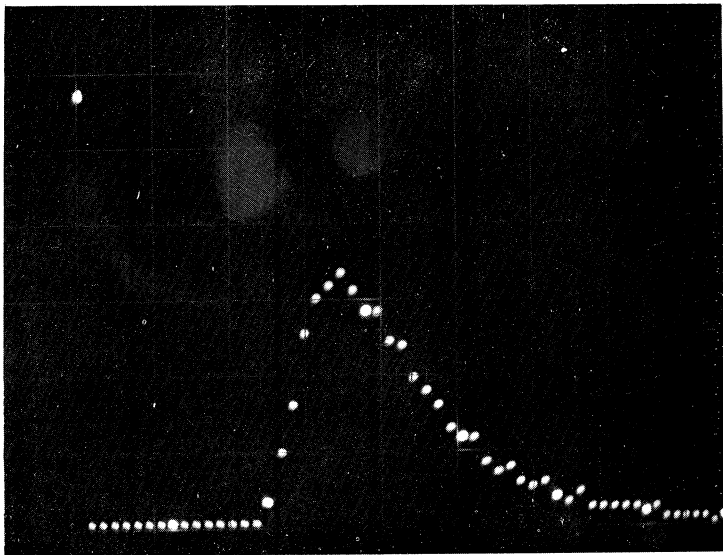
1.5



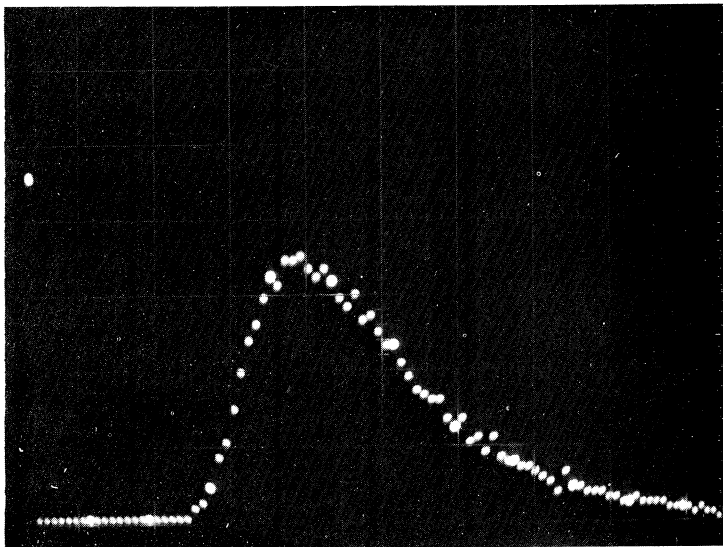
2.0

3084

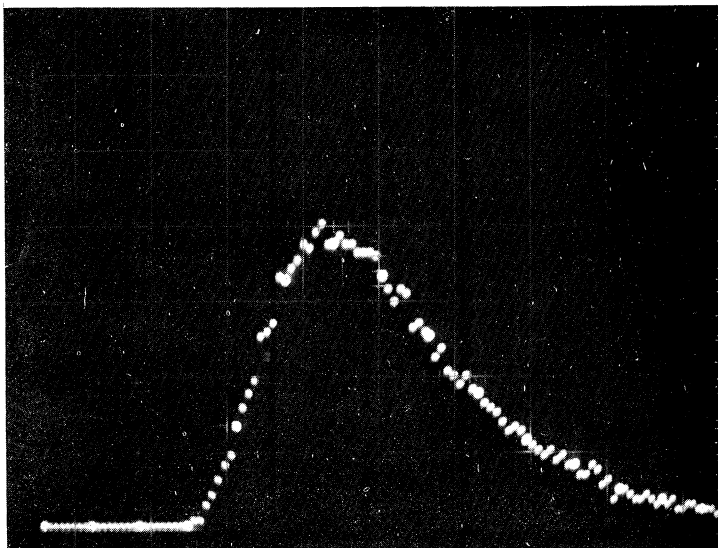
Figure 17. The Size Distribution of Rawweed Particles



Amplifier Gain Setting: 3.5

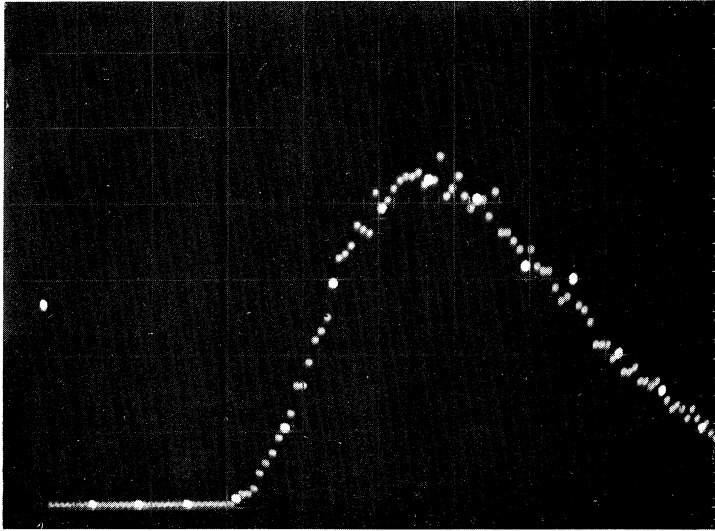


5

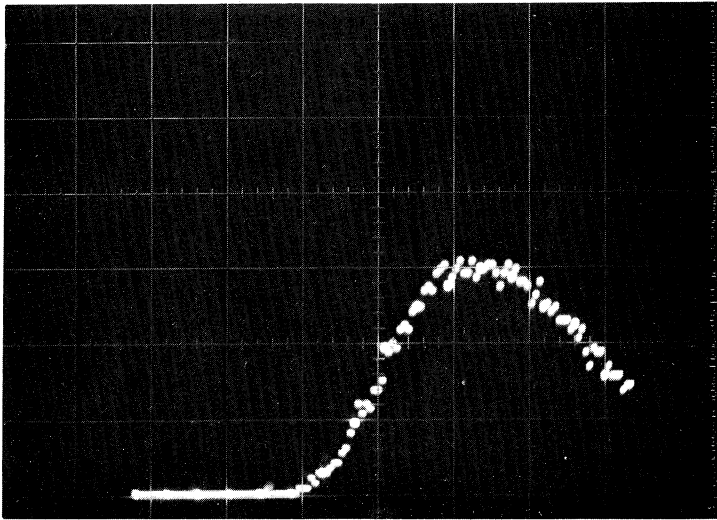


7.5

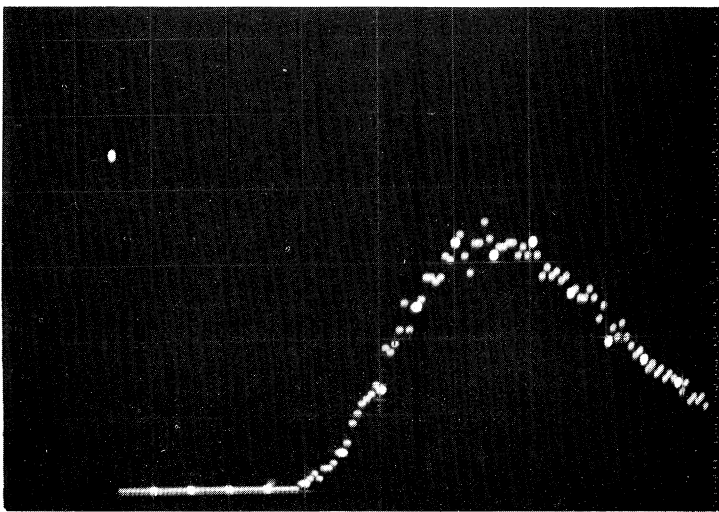
Figure 18a. The Size Distribution of Latex Particles at Different Gain Setting



10



12.5



15

Figure 18b. Continued 3085b

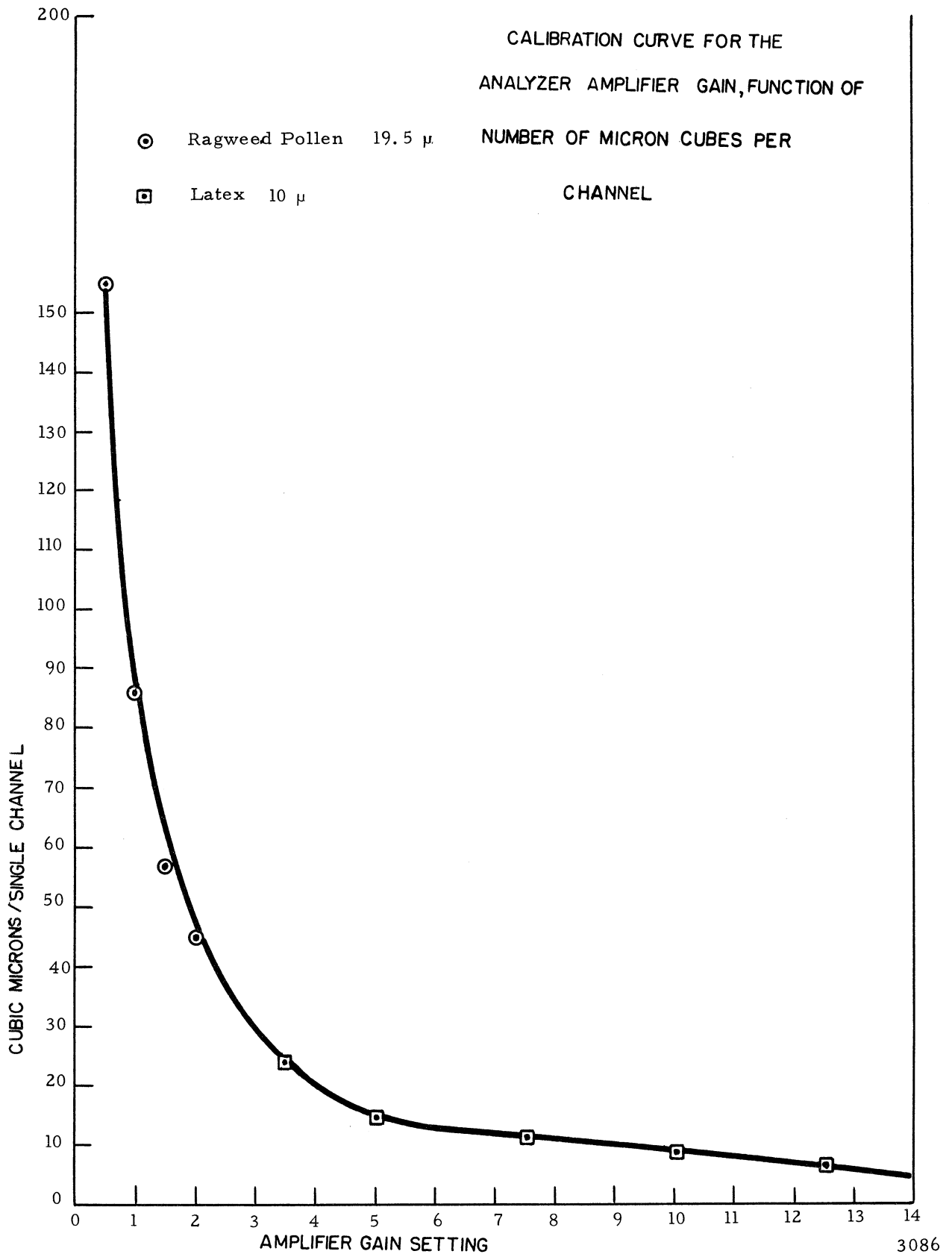
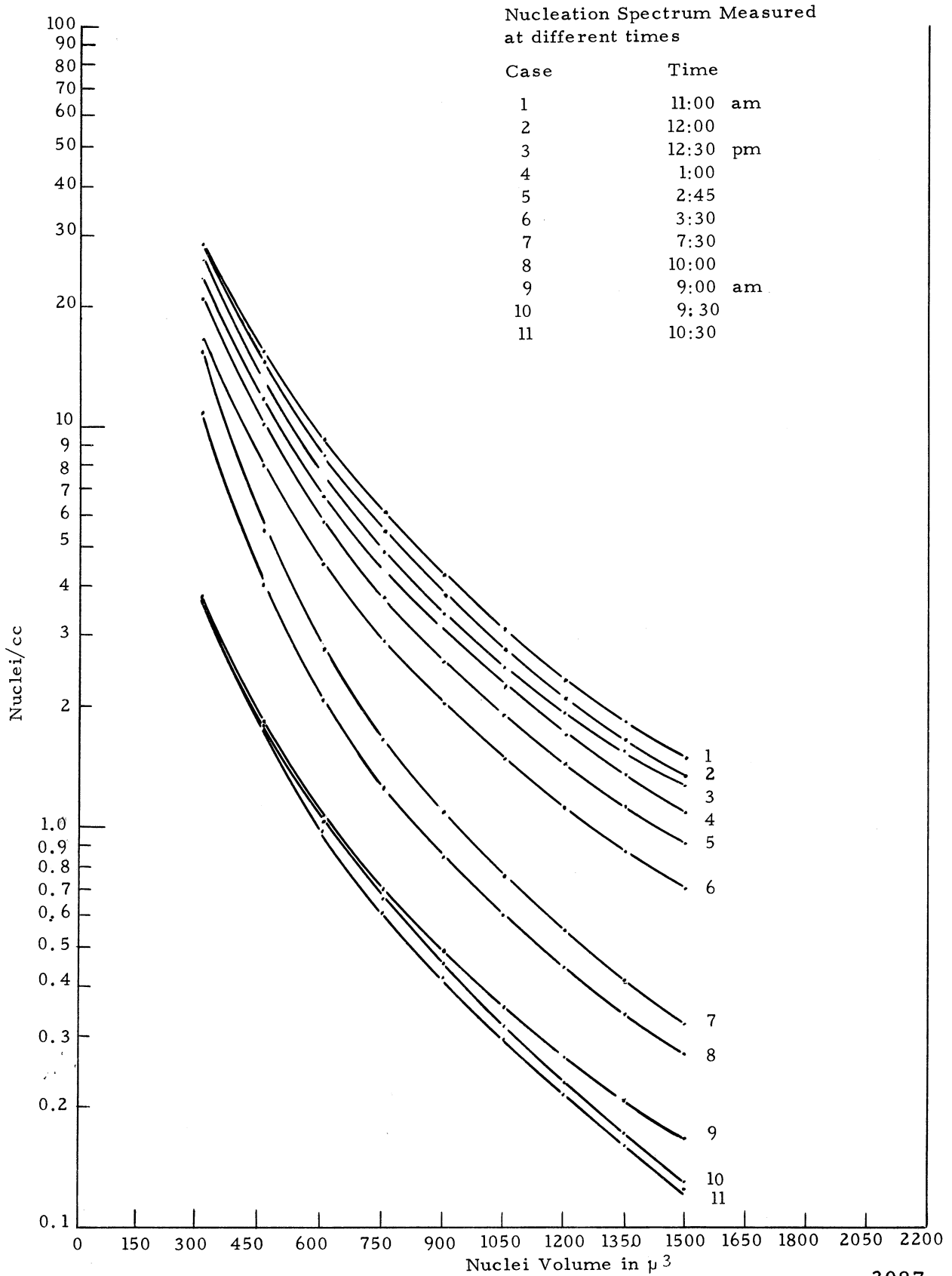


Figure 19. Calibration Curve of the Set-Up for Size Measurements at Different Gain Settings



**Figure 20. Nuclei Size Distribution of the Tunnel Water
at Different Times**

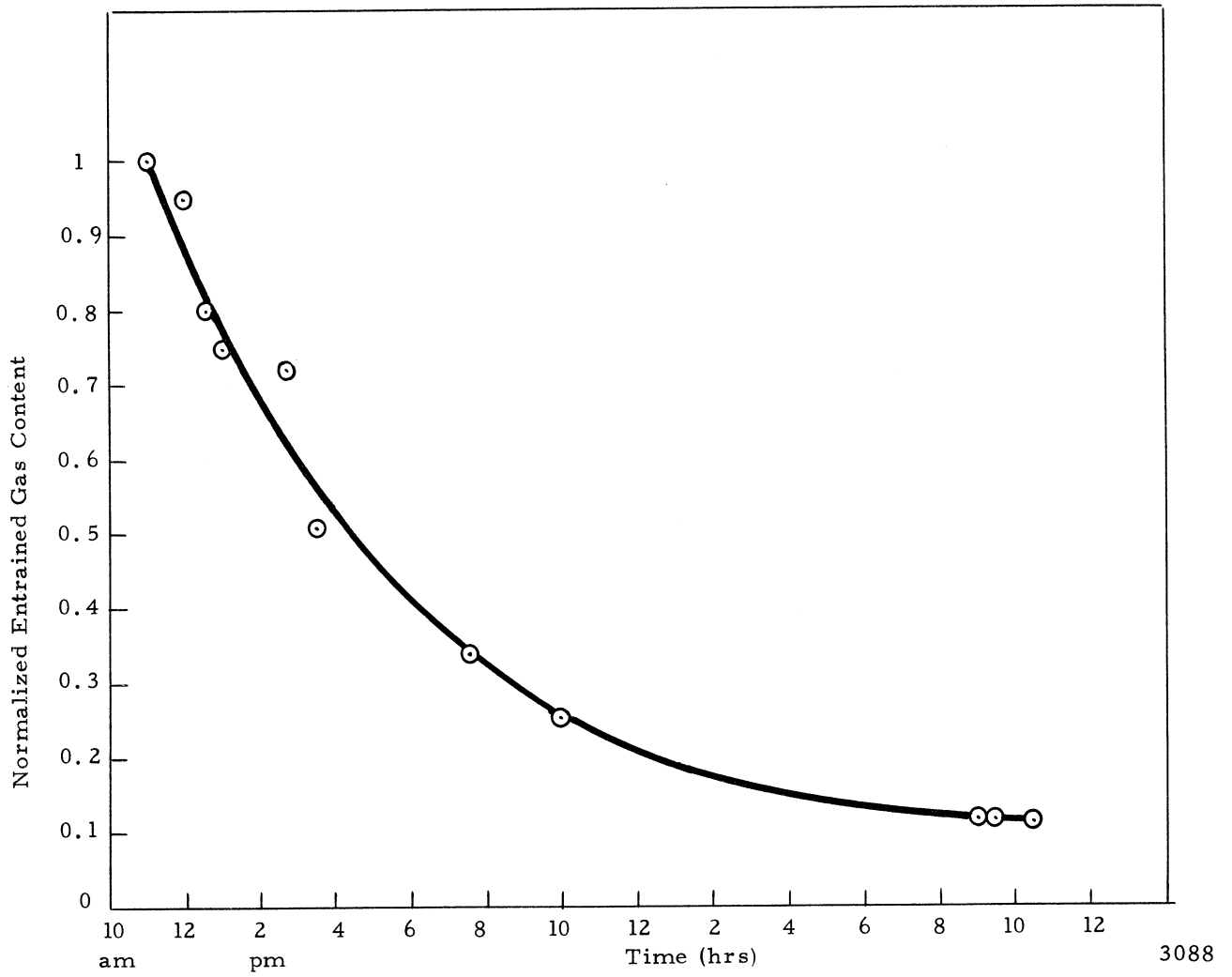


Figure 21. The Entrained Gas Content as a Function of Time